Effect of Biaxial Strain on the Phase Transitions of $Ca(Fe_{1-x}Co_x)_2As_2$

A. E. Böhmer,[1,*] A. Sapkota,[1,2] A. Kreyssig,[1,2] S. L. Bud'ko,[1,2] G. Drachuck,[1,2] S. M. Saunders,[1,2] A. I. Goldman,[1,2] and P. C. Canfield[1,2]

[1]*Ames Laboratory, US DOE, Ames, Iowa 50011, USA*

[2]*Department of Physics and Astronomy, Iowa State University, Ames, Iowa 50011, USA*

(Received 14 November 2016; published 10 March 2017)

We study the effect of applied strain as a physical control parameter for the phase transitions of $Ca(Fe_{1-x}Co_x)_2As_2$ using resistivity, magnetization, x-ray diffraction, and ^{57}Fe Mössbauer spectroscopy. Biaxial strain, namely, compression of the basal plane of the tetragonal unit cell, is created through firm bonding of samples to a rigid substrate via differential thermal expansion. This strain is shown to induce a magnetostructural phase transition in originally paramagnetic samples, and superconductivity in previously nonsuperconducting ones. The magnetostructural transition is gradual as a consequence of using strain instead of pressure or stress as a tuning parameter.

DOI: 10.1103/PhysRevLett.118.107002

Tuning parameters are an essential tool in the study of correlated materials, since they can selectively promote specific interactions. As an example, unconventional superconductivity often emerges around the point where antiferromagnetic order is suppressed by hydrostatic pressure [1]. Strain has been occasionally used as a tuning parameter [2–6], but is less widely employed than pressure. Recently, new piezo-based strain-tuning devices have been presented [7,8] and used in the study of ruthenates [9,10] and SmB_6 [11]. Additionally, strain has been employed to probe the nematic susceptibility of iron-based superconductors [12–16]. Applying strain means enforcing a deformation, or length change with respect to a "free" reference state, and can be achieved using a rigid device. Notably, strain directly affects the electronic band structure and properties. Such enforced deformations depend on fewer elastic constants than deformations achieved by applying force (stress or pressure).

The iron-based superconductors [17–19] sport a complex and highly tunable interplay between antiferromagnetism (AFM), a tetragonal-to-orthorhombic structural distortion, and superconductivity. The variety of suitable tuning parameters includes diverse chemical substitutions [17,20], hydrostatic pressure [17,21,22], epitaxial strain in thin films [23–25], and uniaxial pressure [26–30]. In $Ca(Fe_{1-x}Co_x)_2As_2$, substitution of Co for Fe suppresses a coupled first-order magnetostructural transition at $T_{s,N}$ and induces superconductivity with a maximum T_c of 16 K [31]. $Ca(Fe_{1-x}Co_x)_2As_2$ is exceptionally pressure sensitive [26,27,32,33], as exemplified by the unprecedentedly large rate of suppression of $T_{s,N}$ with hydrostatic pressure, $dT_{s,N}/dp \approx -1100$ K/GPa ($x = 0.028$) [32], 2 orders of magnitude larger than for $BaFe_2As_2$ [34], and by the sensitivity of the material to postgrowth treatment [31,35,36].

Here, we study the effect of strain on $Ca(Fe_{1-x}Co_x)_2As_2$ with a combination of macroscopic and microscopic probes. Biaxial in-plane strain is achieved by making use of the differential thermal expansion between the samples and a rigid substrate, to which the samples are firmly bonded. It directly affects the c/a ratio of the tetragonal samples, similarly to uniaxial pressure along the c direction. In contrast to uniaxial pressure along the tetragonal [110] direction, commonly used for detwinning in iron-based systems [37], it does not break the tetragonal symmetry. We demonstrate that the c/a ratio is a suitable tuning parameter for the phase transitions of $Ca(Fe_{1-x}Co_x)_2As_2$.

Samples of $Ca(Fe_{1-x}Co_x)_2As_2$ ($0 \le x \le 0.054$, with x determined by wavelength dispersive x-ray spectroscopy) were grown out of FeAs flux and annealed at 400 °C, ensuring the absence of the collapsed-tetragonal phase present in as-grown samples [31,35,36]. Samples for resistivity and magnetization measurements were cleaved and cut into small thin bars of typical dimensions of $\sim 1.5 \times 0.2 \times 0.05$ mm^3 and mass of 0.2–0.5 mg. To create strain (ε), samples were glued with Devcon 5-min epoxy to a piece of thin borosilicate glass (Fisherbrand Cover Glass, 160 μm thickness), as shown in the inset to Fig. 1(e). Electrical resistance was measured with an LS370 AC resistance bridge. Magnetic susceptibility was measured under zero-field cooled (ZFC) conditions in a Quantum Design MPMS SQUID magnetometer. ^{57}Fe Mössbauer spectroscopy was performed in transmission using a SEE Co. conventional constant-acceleration-type spectrometer with a ^{57}Co(Rh) source kept at room temperature on a set of ~40 samples [$x = 0.035$, typical dimensions of $2 \times 1 \times (0.04–0.1)$ mm^3]. High-energy (100.3 keV) x-ray diffraction was performed similarly to in Ref. [38], on a strained sample from the Mössbauer set, employing a Pixirad-1 detector. Thermal expansion was also measured with a home-built capacitance dilatometer [39].

Figure 1 shows the normalized resistivity and the ZFC magnetization of a selection of samples with different Co

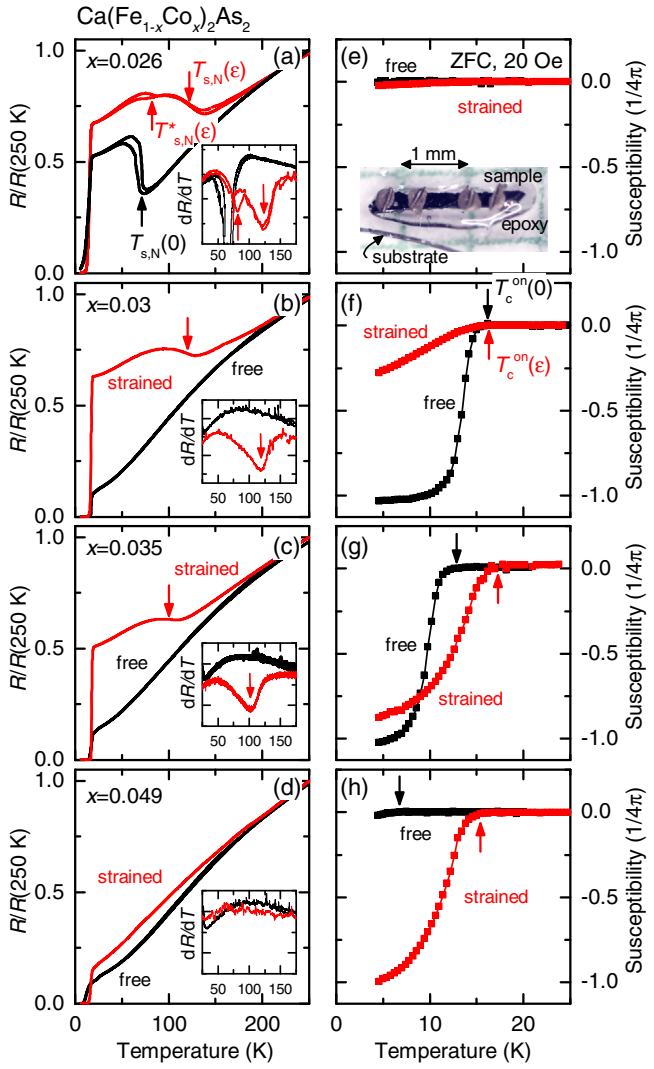

FIG. 1. (a)–(d) Normalized electrical resistivity and (e)–(h) zero-field cooled magnetization (superconducting shielding) of $Ca(Fe_{1-x}Co_x)_2As_2$, with varying Co content x. Measurements were performed on the same thin bar-shaped samples, first free (0) and then strained by gluing to the glass substrate (ε) [photograph in the inset in (e)]. Magnetization was measured parallel to the sample length to minimize demagnetization effects.

concentrations. Each sample was first measured in free-standing (0) and then in strained (ε) conditions to directly reveal the impact of strain. The data on free samples are in very good agreement with previous work [31,36], yet strain induces dramatic changes. For the underdoped ($x = 0.026$) sample, the sharp rise of resistivity at $T_{s,N}(0) \approx 70$ K in the free state, is replaced by a broader anomaly at a higher temperature $T_{s,N}(\varepsilon) \approx 125$ K [defined as the minimum in derivative, insets in Figs. 1(a)–1(c)] and a hysteretic anomaly at $T^*_{s,N}(\varepsilon) \approx 80$ K in the strained state. No significant superconducting shielding fraction is observed in either state, consistent with the mutual exclusion of superconductivity and antiferromagnetism in $Ca(Fe_{1-x}Co_x)_2As_2$ [31]. Freestanding samples having slightly higher Co content, $x = 0.03$ and $x = 0.035$, show no magnetostructural transition and have full superconducting shielding with onset T_c^{on} values of 15.5 and 12 K, respectively. Under strain, clear anomalies in the resistance appear at $T_{s,N}(\varepsilon) = 120$ K and 100 K, respectively, and the superconducting shielding fraction decreases. For the highest Co content ($x = 0.049$), in contrast, the strain induces no high-temperature anomaly. Instead, strain induces full superconducting shielding in this sample that showed only a tiny trace of superconductivity in its free state.

In order to characterize microscopically the strain and the strain-induced resistivity anomalies, we performed high-energy x-ray diffraction on strained $Ca(Fe_{0.965}Co_{0.035})_2As_2$, and compare the results with the uniaxial thermal expansion of free samples as determined by capacitance dilatometry (Fig. 2). The in-plane length of freestanding $Ca(Fe_{0.965}Co_{0.035})_2As_2$ [solid grey line in Fig. 2(a)] increases strongly upon decreasing temperature, whereas the thermal expansion of the glass substrate is fairly low (solid blue line). The diffraction data show that the in-plane axis of strained $Ca(Fe_{0.965}Co_{0.035})_2As_2$ follows the substrate length rather closely, which means that it is compressed with respect to the freestanding state for $T \gtrsim 100$ K. As seen from Fig. 2(b), the strained sample's c axis is expanded with respect to its length in the freestanding state, as is expected from the Poisson effect [40]. Thus, the imposed strain corresponds to an elongation of the tetragonal unit cell, by $[L_{a,b}(\varepsilon) - L_{a,b}(0)]/L_{a,b}(0) \sim -0.3\%$ and $[L_c(\varepsilon) - L_c(0)]/L_c(0) \sim 0.55\%$ at 105 K, as shown schematically in the right inset of Fig. 2(a).

Because the high-energy x rays penetrate the entire sample thickness, the strain distribution may be inferred from the diffraction data (color maps in Fig. 2). The narrow intensity distribution around $a = 5.51$ Å at 105 K implies homogeneous strain in the $\sim 1 \times 10^{-3}$ mm^3 sample volume illuminated by the 0.1×0.1 mm^2 x-ray beam, oriented perpendicular to the sample surface. In the c-axis measurement [(0 0 10) reflection] the intensity is peaked around $c = 11.52$ Å at 105 K but has a tail towards lower values, indicating that a fraction of the $\sim 1 \times 10^{-2}$ mm^3 sample volume illuminated by the beam at the small angle of $\sim 5°$ experiences reduced strain.

The tetragonal-to-orthorhombic (T-to-OR) structural transition is obvious from the split of the in-plane lattice parameter into a_{OR} and b_{OR} in Fig. 2(a) and is, in more detail, shown by the splitting of the tetragonal (6 6 0) reflection, similar to what is seen in AFe_2As_2 (A = Ba, Sr, Ca) parent compounds [41]. Note that a globally firm bonding between sample and substrate at all temperatures is supported by the observation that the center of the diffraction pattern, i.e., the average in-plane length of the sample as inferred from x-ray diffraction, follows the substrate length quite closely.

A peculiarity is that in the strained $x = 0.035$ sample, two phase fractions coexist from 105 K down to the lowest temperature, as clearly visible in the c-axis diffraction data. The "transformed" OR phase fraction, f_{OR}, has a

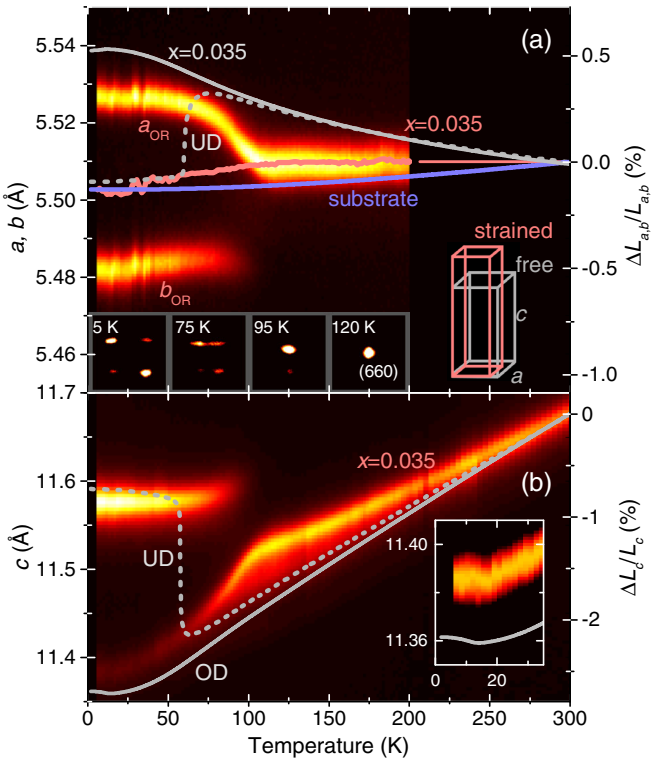

FIG. 2. (a) In-plane and (b) c-axis structural data for $Ca(Fe_{1-x}Co_x)_2As_2$. Lattice parameters of strained $Ca(Fe_{0.965}Co_{0.035})_2As_2$ from x-ray diffraction measured on warming are shown as color-coded intensity maps (left axis). Lines indicate uniaxial fractional length changes, $\Delta L_i/L_i$ ($i = c$, c axis and $i = a$, b, in-plane average), of free overdoped (OD) samples [(a) $x = 0.035$ (this work) and (b) $x = 0.029$ [33]] and of a representative underdoped (UD) $x = 0.027$ sample [33] obtained by capacitance dilatometry [right axis, scaled so that $\Delta L_c/L_c$ corresponds to the lattice parameter change $[c(T) - c(300\ \mathrm{K})]/c(300\ \mathrm{K})$ in (b) and analogously in (a)]. The blue line in (a) shows the substrate thermal expansion and the red line indicates the average in-plane length of strained $Ca(Fe_{0.965}Co_{0.035})_2As_2$ inferred from the diffraction data. The right inset in (a) depicts schematically the deformation of the unit cell in the strained state. The row of insets in (a) shows the $(HK0)$ diffraction pattern close to the tetragonal (660) reflection revealing orthorhombic domains. The inset in (b) presents the data on expanded scales.

significantly larger c-lattice parameter, comparable to the increase of the c axis of free underdoped samples on entering the OR-AFM phase. The "remaining" T phase fraction has a smaller c-lattice parameter, which appears to exhibit a small kink at ~15 K [visualized in the inset to Fig. 2(b)], reminiscent of the signature of bulk superconductivity in free overdoped samples [33].

The following simplified picture likely explains the peculiarities of the strain-induced first-order transition in our samples. Firm bonding to the rigid substrate forces the in-plane sample length L_{sample} to be equal to a length $L_{\mathrm{substrate}}$. On decreasing temperature, the sample experiences increasing strain: the basal plane is compressed, and the c axis expands relative to the free state. This kind of deformation favors the OR phase thermodynamically, since its average in-plane length, L_{OR}, is smaller than in the T phase (L_{T}), and its c-axis length is larger (dashed lines in Fig. 2) [33]. At a critical temperature or value of strain, the OR phase nucleates in some parts of the sample. Those transformed parts have a reduced in-plane area so that some of the strain is released. Hence, the remaining T phase can partly relax its lattice parameters and does not transform. The boundary condition is expressed by $L_{\mathrm{sample}} = f_{\mathrm{OR}}L_{\mathrm{OR}} + (1 - f_{\mathrm{OR}})L_{\mathrm{T}} = L_{\mathrm{substrate}}$ and, if $L_{\mathrm{OR}} < L_{\mathrm{substrate}} < L_{\mathrm{T}}$, a solution that balances the free energies of the T and the OR phases, and the elastic energy of the lattice deformations, likely entails $0 < f_{\mathrm{OR}} < 1$. As a consequence, there is a well-defined phase coexistence and f_{OR} changes gradually with temperature. Note that such a phase coexistence implies locally inhomogeneous strain.

The relaxation of the lattice parameters of the remaining T phase below the onset of the transition is clearly visible as kinks in the diffraction data around ~100 K. The a axis of the remaining T phase follows rather closely the orthorhombic a_{OR} axis, and is, therefore, not distinctly visible at low temperatures. Finally, for underdoped samples, the yet-untransformed phase fraction will naturally undergo the AFM-OR transition on its own close to the transition temperature under freestanding conditions, which explains the second anomaly, at $T^*_{s,N}(\varepsilon) \approx T_{s,N}(0)$, in resistivity in Fig. 1(a).

Whether the induced OR phase in strained $Ca(Fe_{0.965}Co_{0.035})_2As_2$ is also magnetically ordered is studied using ^{57}Fe Mössbauer spectroscopy, a local probe of the ordered magnetic hyperfine field (Fig. 3). The doublet-type spectrum measured on free samples (attached to the glass substrate with Apiezon N grease) confirms their paramagnetic ground state. In contrast, when the same samples are glued with epoxy to the glass substrate and thus strained, the spectrum is given by a superposition of a paramagnetic doublet and a magnetic sextet. The relative areas indicate that a fraction of $f_{\mathrm{AFM}} \approx 80\%$ of the Fe nuclei experience a distinct magnetic hyperfine field at low temperatures. On increasing temperature, a purely paramagnetic state is recovered at 125 K. Figures 3(d)–3(e) summarize the obtained structural distortion and magnetic hyperfine field, as well as the respective ordered phase fractions. The low-temperature values of both the magnetic hyperfine field H_{hf} and orthorhombic distortion δ are only ~20% lower than the values of pure $CaFe_2As_2$, namely, $H_{\mathrm{hf}} = 10$ T [35] and $\delta(0) = 5 \times 10^{-3}$ [42]. In addition, $\delta(T)$ and $H_{\mathrm{hf}}(T)$ follow each other closely, indicating that a coupled first-order magnetostructural transition is indeed induced by the strain.

The phase diagram in Fig. 4 is constructed from the resistivity and magnetization data. The superconducting shielding fractions are presented as color-coded maps in Figs. 4(b) and 4(c). In agreement with previous reports

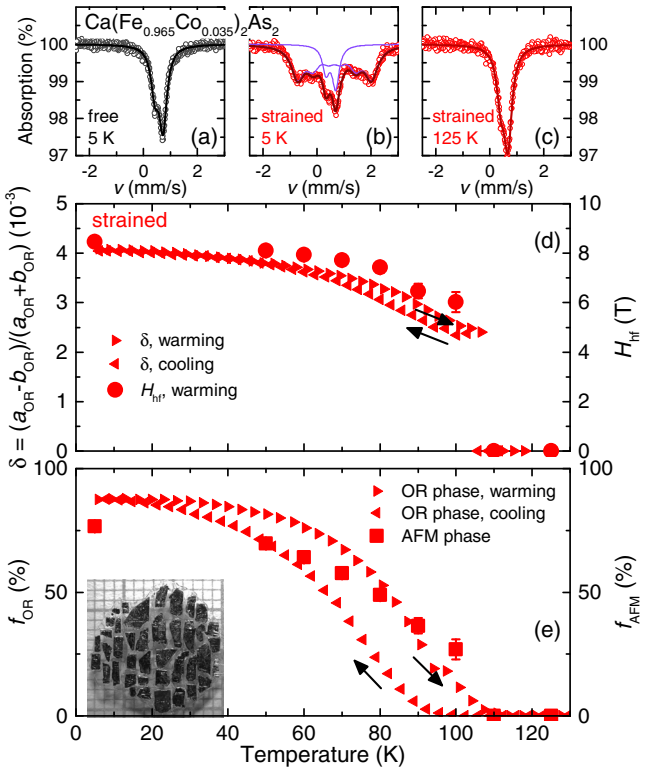

FIG. 3. (a)–(c) Examples of ^{57}Fe Mössbauer spectra of $Ca(Fe_{0.965}Co_{0.035})_2As_2$ (symbols) and the fitted paramagnetic doublet and magnetic sextet (lines). (d) Orthorhombic order parameter $\delta = (a_{OR} - b_{OR})/(a_{OR} + b_{OR})$ and magnetic hyperfine field H_{hf}. (e) AFM and OR phase fractions, f_{AFM} and f_{OR}, respectively. f_{AFM}, deduced from Mössbauer spectroscopy (which probes the whole sample mosaic), reaches a maximum of ~80%, and f_{OR}, deduced from c-axis x-ray diffraction (which probes only a part of the same), reaches ~90%. Diffraction reveals a temperature hysteresis, whereas Mössbauer spectroscopy was performed only on warming. The inset shows a photograph of the samples used for these measurements on a mm grid.

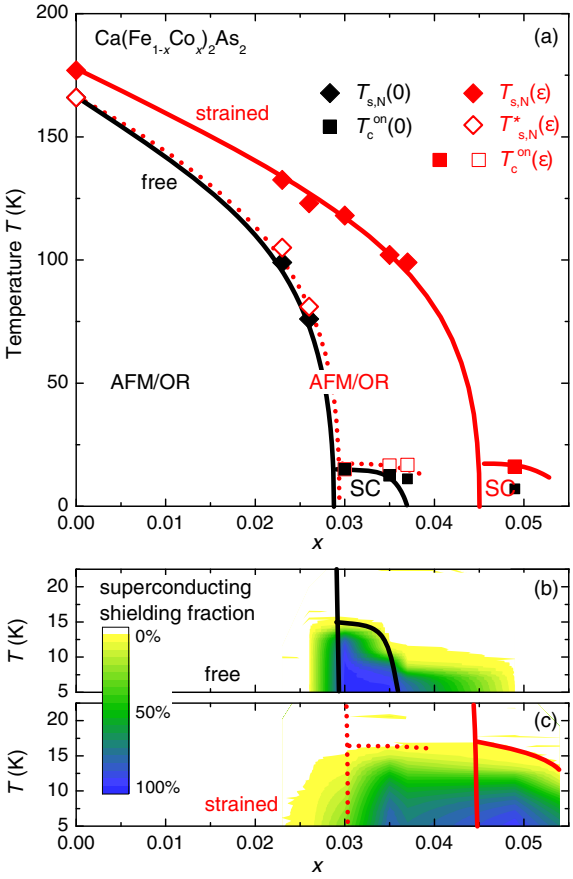

FIG. 4. (a) Phase diagram of $Ca(Fe_{1-x}Co_x)_2As_2$ in the free (black) and strained (red) state with increased c/a ratio. The AFM-OR transition at $T_{s,N}(\varepsilon)$ is only gradual. Red open symbols and dashed lines correspond to the remaining phase fraction within the strained sample. (b),(c) Superconducting shielding fraction of free and strained samples, respectively. Lines are a guide to the eye.

[31], freestanding samples show a steep doping-induced suppression of the magnetostructural transition at $x \approx 0.028$ and a superconducting half dome between $x = 0.03$–0.035. The strained samples exhibit a significantly extended range of the AFM-OR phase, as confirmed by the microscopic probes. The superconducting shielding is reduced in this range and full shielding is reached only for $x = 0.049$. Hence, the superconducting dome is less sharply defined than for free samples. This is a natural consequence of the phase coexistence under strain. At low temperatures, the remaining tetragonal phase fraction becomes superconducting, while the OR phase fraction likely stays nonsuperconducting. Note that the ZFC shielding fraction may overestimate the true superconducting volume fraction.

In summary, increasing the c/a ratio through applying biaxial strain shifts the phase diagram of $Ca(Fe_{1-x}Co_x)_2As_2$ to higher x, without a change of the maximum T_c. This suggests the possibility that the maximum T_c in this system has already been reached. In general, the initial rate of change of transition temperatures with uniaxial pressure can be inferred from thermodynamic relations, using, in particular, uniaxial thermal expansion. The trends inferred for $Ca(Fe_{1-x}Co_x)_2As_2$ [32,33] agree with the present result, whereas a quantitative estimate that takes into account the compressibility of the material agrees within a factor of ~2–3. Notably, in most iron-based systems, uniaxial pressure derivatives have opposite sign along the a and c axes [30,33,43], indicating that these systems are notably more sensitive to changes of the c/a ratio than to hydrostatic pressure, which averages those components and entails partial cancellation of opposing effects. As studied in detail in $BaFe_2As_2$, however, the relation between the phase diagram and changes of the c/a ratio, when achieved either by pressure or by substitution with various transition metals, is nonuniversal [44,45].

This strain tuning is analogous to epitaxial strain in thin films, which was recently studied in thin films of $Ba(Fe_{1-x}Co_x)_2As_2$ grown on different substrates. An in-plane strain of almost $\pm 0.6\%$ was achieved and yielded changes of T_N and T_c of $\lesssim 10$ K [25]. The changes are very

similar to the present result, considering a lower strain sensitivity of $BaFe_2As_2$ with respect to $CaFe_2As_2$. The magnitude of applied strain in the present study depends on temperature and on the difference in thermal expansivity between sample and substrate. We expect that $BaFe_2As_2$ rigidly glued to our glass substrate experiences only $\sim -0.02\%$ of in-plane strain at $T_{s,N} = 140$ K, but $\sim -0.12\%$ when a copper substrate is used. This should result in a small but measurable shift of $T_{s,N}$ by 1–2 K. The effect on T_c of optimally doped $Ba(Fe_{1-x}Co_x)_2As_2$ is likely of similar size.

At any strain-induced first-order phase transition, however, the change of lattice parameters will result in (partial) strain release and a well-defined phase coexistence, similar to our observations. In this respect, controlling the total sample length is fundamentally different from controlling stress or pressure. This has implications for other techniques utilizing strain and needs to be taken into account when gluing thin samples to a rigid substrate, which is a common practice in a variety of experimental techniques.

In conclusion, biaxial strain is established as a tuning parameter for the phase transitions of bulk $Ca(Fe_{1-x}Co_x)_2As_2$. Although the observed strain effects are particularly pronounced in the extremely sensitive $CaFe_2As_2$ system, they can occur in principle in any material.

We are grateful to D. S. Robinson for the excellent support of the x-ray diffraction measurements and to Valentin Taufour, Makariy Tanatar, and Herman Suderow for helpful discussions. This work was supported by the U.S. Department of Energy (DOE), Office of Basic Energy Science, Division of Materials Sciences and Engineering. Ames Laboratory is operated for the DOE by Iowa State University under Contract No. DE-AC02-07CH11358. A. E. B. acknowledges support from the Helmholtz Association via Grant No. PD-226. G. D. and S. M. S. were supported by the Gordon and Betty Moore Foundation's EPiQS Initiative through Grant No. GBMF4411. This research used resources of the Advanced Photon Source, a DOE Office of Science User Facility operated for the DOE Office of Science by Argonne National Laboratory under Contract No. DE-AC02-06CH11357.

*Corresponding author.
boehmer@ameslab.gov

[1] Y. J. Uemura, Superconductivity: Commonalities in phase and mode, Nat. Mater. **8**, 253 (2009).
[2] M. J. Skove, E. P. Stillwell, and J. H. Davis, Two "whisker" straining devices suitable for low temperatures, Rev. Sci. Instrum. **39**, 155 (1968).
[3] D. R. Overcash, M. J. Skove, and E. P. Stillwell, Effect of elastic stress on some electronic properties of indium, Phys. Rev. **187**, 570 (1969).
[4] M. A. Angadi, D. E. Britton, and E. Fawcett, Low temperature sample holder for rotating a crystal under tension in a superconducting soleniod, J. Phys. E **6**, 1086 (1973).
[5] Yu. P. Gaĭdukov, N. P. Danilova, and M. B. Shcherbina-Saimoĭlova, Phase transition of order 2 1/2 in zinc, Pis'ma Zh. Eksp. Teor. Fiz. **25**, 509 (1977) [JETP Lett. **25**, 479 (1977)].
[6] M. Shayegan, K. Karrai, Y. P. Shkolnikov, K. Vakili, E. P. De Poortere, and S. Manus, Low-temperature, in situ tunable, uniaxial stress measurements in semiconductors using a piezoelectric actuator, Appl. Phys. Lett. **83**, 5235 (2003).
[7] C. W. Hicks, M. E. Barber, S. D. Edkins, D. O. Brodsky, and A. P. Mackenzie, Piezoelectric-based apparatus for strain tuning, Rev. Sci. Instrum. **85**, 065003 (2014).
[8] L. Gannon, A. Bosak, R. G. Burkovsky, G. Nisbet, A. P. Petrovi, and M. Hoesch, A device for the application of uniaxial strain to single crystal samples for use in synchrotron radiation experiments, Rev. Sci. Instrum. **86**, 103904 (2015).
[9] C. W. Hicks, D. O. Brodsky, E. A. Yelland, A. S. Gibbs, J. A. N. Bruin, M. E. Barber, S. D. Edkins, K. Nishimura, S. Yonezawa, Y. Maeno, and A. P. Mackenzie, Strong increase of T_c of Sr_2RuO_4 under both tensile and compressive strain, Science **344**, 283 (2014).
[10] A. Steppke, L. Zhao, M. E. Barber, T. Scaffidi, F. Jerzembeck, H. Rosner, A. S. Gibbs, Y. Maeno, S. H. Simon, A. P. Mackenzie, and C. W. Hicks, Strong peak in T_c of Sr_2RuO_4 under uniaxial pressure, Science **355**, 6321 (2017).
[11] A. Stern, M. Dzero, V. M. Galitski, Z. Fisk, and J. Xia, Kondo insulator SmB_6 under strain: Surface dominated conduction near room temperature, arXiv:1607.07454.
[12] J.-H. Chu, H.-H. Kuo, J. G. Analytis, and I. R. Fisher, Divergent nematic susceptibility in an iron arsenide superconductor, Science **337**, 710 (2012).
[13] H.-H. Kuo, M. C. Shapiro, S. C. Riggs, and I. R. Fisher, Measurement of the elastoresistivity coefficients of the underdoped iron arsenide $Ba(Fe_{0.975}Co_{0.025})_2As_2$, Phys. Rev. B **88**, 085113 (2013).
[14] H.-H. Kuo, J.-H. Chu, J. C. Palmstrom, S. A. Kivelson, and I. R. Fisher, Ubiquitous signatures of nematic quantum criticality in optimally doped Fe-based superconductors, Science **352**, 958 (2016).
[15] M. C. Shapiro, P. Hlobil, A. T. Hristov, A V. Maharaj, and I. R. Fisher, Symmetry constraints on the elastoresistivity tensor, Phys. Rev. B **92**, 235147 (2015).
[16] M. He, L. Wang, F. Ahn, F. Hardy, T. Wolf, P. Adelmann, J. Schmalian, I. Eremin, and C. Meingast, Dichotomy between in-plane magnetic susceptibility and resistivity anisotropies in extremely strained $BaFe_2As_2$, arXiv:1610.05575.
[17] P. C. Canfield and S. L. Bud'ko, FeAs-based superconductivity: A case study of the effects of transition metal doping on $BaFe_2As_2$, Annu. Rev. Condens. Matter Phys. **1**, 27 (2010).
[18] D. C. Johnston, The puzzle of high temperature superconductivity in layered iron pnictides and chalcogenides, Adv. Phys. **59**, 803 (2010).
[19] Q. Si, R. Yu, and E. Abrahams, High-temperature superconductivity in iron pnictides and chalcogenides, Nat. Rev. Mater. **1**, 16017 (2016).
[20] M. Merz, P. Schweiss, P. Nagel, M.-J. Huang, R. Eder, T. Wolf, H. von Löhneysen, and S. Schuppler, Of substitution and doping: Spatial and electronic structure in Fe pnictides, J. Phys. Soc. Jpn. **85**, 044707 (2016).

[21] H. Takahashi, K. Igawa, K. Arii, Y. Kamihara, M. Hirano, and H. Hosono, Superconductivity at 43 K in an iron-based layered compound $LaO_{1-x}F_xFeAs$, Nature (London) **453**, 376 (2008).

[22] A. S. Sefat, Pressure effects on two superconducting iron-based families, Rep. Prog. Phys. **74**, 124502 (2011).

[23] K. Iida, J. Hänisch, R. Hühne, F. Kurth, M. Kidszun, S. Haindl, J. Werner, L. Schultz, and B. Holzapfel, Strong T_c dependence for strained epitaxial $Ba(Fe_{1-x}Co_x)_2As_2$ thin films, Appl. Phys. Lett. **95**, 192501 (2009).

[24] J. Engelmann, V. Grinenko, P. Chekhonin, W. Skrotzki, D. V. Efremov, S. Oswald, K. Iida, R. Hühne, J. Hänisch, M. Hoffmann, F. Kurth, L. Schultz, and B. Holzapfel, Strain induced superconductivity in the parent compound $BaFe_2As_2$, Nat. Commun. **4**, 2877 (2013).

[25] K. Iida, V. Grinenko, F. Kurth, A. Ichinose, I. Tsukada, E. Ahrens, A. Pukenas, P. Chekhonin, W. Skrotzki, A. Teresiak, R. Hühne, S. Aswartham, S. Wurmehl, I. Mönch, M. Erbe, J. Hänisch, B. Holzapfel, S.-L. Drechsler, and D. V. Efremov, Hall-plot of the phase diagram for $Ba(Fe_{1-x}Co_x)_2As_2$, Sci. Rep. **6**, 28390 (2016).

[26] M. S. Torikachvili, S. L. Bud'ko, N. Ni, P. C. Canfield, and S. T. Hannahs, Effect of pressure on transport and magneto-transport properties in $CaFe_2As_2$ single crystals, Phys. Rev. B **80**, 014521 (2009).

[27] K. Prokeš, A. Kreyssig, B. Ouladdiaf, D. K. Pratt, N. Ni, S. L. Bud'ko, P. C. Canfield, R. J. McQueeney, D. N. Argyriou, and A. I. Goldman, Evidence from neutron diffraction for superconductivity in the stabilized tetragonal phase of $CaFe_2As_2$ under uniaxial pressure, Phys. Rev. B **81**, 180506 (2010).

[28] S. L. Bud'ko, N. Ni, S. Nandi, G. M. Schmiedeshoff, and P. C. Canfield, Thermal expansion and anisotropic pressure derivatives of T_c in $Ba(Fe_{1-x}Co_x)_2As_2$ single crystals, Phys. Rev. B **79**, 054525 (2009).

[29] T. Yamazaki, N. Takeshita, R. Kobayashi, H. Fukazawa, Y. Kohori, K. Kihou, C.-H. Lee, H. Kito, A. Iyo, and H. Eisaki, Appearance of pressure-induced superconductivity in $BaFe_2As_2$ under hydrostatic conditions and its extremely high sensitivity to uniaxial stress, Phys. Rev. B **81**, 224511 (2010).

[30] C. Meingast, F. Hardy, R. Heid, P. Adelmann, A. Böhmer, P. Burger, D. Ernst, R. Fromknecht, P. Schweiss, and T. Wolf, Thermal Expansion and Grüneisen Parameters of $Ba(Fe_{1-x}Co_x)_2As_2$: A Thermodynamic Quest for Quantum Criticality, Phys. Rev. Lett. **108**, 177004 (2012).

[31] S. Ran, S. L. Bud'ko, W. E. Straszheim, J. Soh, M. G. Kim, A. Kreyssig, A. I. Goldman, and P. C. Canfield, Control of magnetic, nonmagnetic, and superconducting states in annealed $Ca(Fe_{1-x}Co_x)_2As_2$, Phys. Rev. B **85**, 224528 (2012).

[32] E. Gati, S. Köhler, D. Guterding, B. Wolf, S. Knöner, S. Ran, S. L. Bud'ko, P. C. Canfield, and M. Lang, Hydrostatic-pressure tuning of magnetic, nonmagnetic, and superconducting states in annealed $Ca(Fe_{1-x}Co_x)_2As_2$, Phys. Rev. B **86**, 220511 (2012).

[33] S. L. Bud'ko, S. Ran, and P. C. Canfield, Thermal expansion of $CaFe_2As_2$: Effect of cobalt doping and postgrowth thermal treatment, Phys. Rev. B **88**, 064513 (2013).

[34] E. Colombier, S. L. Bud'ko, N. Ni, and P. C. Canfield, Complete pressure-dependent phase diagrams for $SrFe_2As_2$ and $BaFe_2As_2$, Phys. Rev. B **79**, 224518 (2009).

[35] S. Ran, S. L. Bud'ko, D. K. Pratt, A. Kreyssig, M. G. Kim, M. J. Kramer, D. H. Ryan, W. N. Rowan-Weetaluktuk, Y. Furukawa, B. Roy, A. I. Goldman, and P. C. Canfield, Stabilization of an ambient-pressure collapsed tetragonal phase in $CaFe_2As_2$ and tuning of the orthorhombic-antiferromagnetic transition temperature by over 70 K via control of nanoscale precipitates, Phys. Rev. B **83**, 144517 (2011).

[36] S. Ran, Ph. D. thesis, Iowa State University, 2014.

[37] I. R. Fisher, L. Degiorgi, and Z. X. Shen, In-plane electronic anisotropy of underdoped '122' Fe-arsenide superconductors revealed by measurements of detwinned single crystals, Rep. Prog. Phys. **74**, 124506 (2011).

[38] A. Sapkota, G. S. Tucker, M. Ramazanoglu, W. Tian, N. Ni, R. J. Cava, R. J. McQueeney, A. I. Goldman, and A. Kreyssig, Lattice distortion and stripelike antiferromagnetic order in $Ca_{10}(Pt_3As_8)(Fe_2As_2)_5$, Phys. Rev. B **90**, 100504 (2014).

[39] G. M. Schmiedeshoff, A. W. Lounsbury, D. J. Luna, S. J. Tracy, A. J. Schramm, S. W. Tozer, V. F. Correa, S. T. Hannahs, T. P. Murphy, E. C. Palm, A. H. Lacerda, S. L. Budko, P. C. Canfield, J. L. Smith, J. C. Lashley, and J. C. Cooley, Versatile and compact capacitive dilatometer, Rev. Sci. Instrum. **77**, 123907 (2006).

[40] M. Tomić, R. Valentí, and H. O. Jeschke, Uniaxial versus hydrostatic pressure-induced phase transitions in $CaFe_2As_2$ and $BaFe_2As_2$, Phys. Rev. B **85**, 094105 (2012).

[41] M. A. Tanatar, A. Kreyssig, S. Nandi, N. Ni, S. L. Bud'ko, P. C. Canfield, A. I. Goldman, and R. Prozorov, Direct imaging of the structural domains in the iron pnictides AFe_2As_2 (A = Ca, Sr, Ba), Phys. Rev. B **79**, 180508 (2009).

[42] A. I. Goldman, D. N. Argyriou, B. Ouladdiaf, T. Chatterji, A. Kreyssig, S. Nandi, N. Ni, S. L. Bud'ko, P. C. Canfield, and R. J. McQueeney, Lattice and magnetic instabilities in $CaFe_2As_2$: A single-crystal neutron diffraction study, Phys. Rev. B **78**, 100506 (2008).

[43] A. E. Böhmer, F. Hardy, L. Wang, T. Wolf, P. Schweiss, and C. Meingast, Superconductivity-induced reentrance of orthorhombic distortion in $Ba_{1-x}K_xFe_2As_2$, Nat. Commun. **6**, 7911 (2015).

[44] N. Ni, A. Thaler, A. Kracher, J. Q. Yan, S. L. Bud'ko, and P. C. Canfield, Phase diagrams of $Ba(Fe_{1-x}M_x)_2As_2$ single crystals (M = Rh and Pd), Phys. Rev. B **80**, 024511 (2009).

[45] A. Thaler, N. Ni, A. Kracher, J. Q. Yan, S. L. Bud'ko, and P. C. Canfield, Physical and magnetic properties of $Ba(Fe_{1-x}Ru_x)_2As_2$ single crystals, Phys. Rev. B **82**, 014534 (2010).